Theoretical study of multinucleon transfer reactions by coupling the Langevin dynamics iteratively with the master equation

F. C. Dai,[1,2] P. W. Wen,[3,*] C. J. Lin,[3,4,†] J. J. Liu,[1] X. X. Xu,[1,2,5,‡] K. L. Wang,[1] H. M. Jia,[3] L. Yang,[3] N. R. Ma,[3] and F. Yang[3]

[1]*Institute of Modern Physics, Chinese Academy of Sciences, Lanzhou 730000, China*
[2]*University of Chinese Academy of Sciences, Beijing 100049, China*
[3]*China Institute of Atomic Energy, Beijing 102413, China*
[4]*College of Physics and Technology and Guangxi Key Laboratory of Nuclear Physics and Technology, Guangxi Normal University, Guilin 541004, China*
[5]*Advanced Energy Science and Technology Guangdong Laboratory, Huizhou 516003, China*

(Received 19 November 2023; accepted 22 January 2024; published 26 February 2024)

Multinucleon transfer (MNT) reactions have received increasing interest in the synthesis of neutron-rich nuclei due to the distinct limitations of other reactions, particularly in the $N = 126$ region, which represents the last waiting point of astrophysical nucleosynthesis. However, it is still a challenging endeavor to describe the MNT process between heavy nuclei. In this study, we develop a theoretical framework that couples the Langevin dynamics iteratively with the master equation, which is based on the HICOL model (CLIM-H). The random transfer process is achieved by solving the master equation using the Monte Carlo method, where the parametric transfer probability with a Q window is employed. The isotope distributions for ^{58,64}Ni + ^{208}Pb, as well as the angular and isotope distributions of the recently measured ^{206}Pb + ^{118}Sn, could be generally reproduced based on this method. Contrary to previous theoretical predictions which show a high production cross section of $N = 126$ nuclei, current calculations do not reveal appreciable cross sections. The distinguishing characteristic of this approach is its ability to generate not only the mass distribution but also the charge distribution self-consistently, which could provide references for many other studies using the multidimensional Langevin equation considering only the mass asymmetry degree of freedom.

DOI: 10.1103/PhysRevC.109.024617

I. INTRODUCTION

There is still an open problem about the natural origins of nuclei heavier than iron. In astrophysical nucleosynthesis, it is now widely supposed that the rapid neutron capture process (r-process) leads the production of nuclei to shift to the right and upwards on the chart of the nuclides until closed neutron shells ($N = 50$, 82, and 126) are present. The closed neutron shell, $N = 126$, as the last waiting point in the r-process, plays an essential role in this process. Meanwhile, there is an expectation in heavy neutron-rich nuclei that the energy levels of single-particle states will noticeably change, which may result in the emergence of new magic numbers [1].

As the exclusive means of synthesizing superheavy nuclei and $N = 126$ neutron-rich nuclei, recent years have witnessed a rise in interest in the multinucleon transfer (MNT) reaction [2–4]. In most cases, the MNT reaction is understood to be a damped binary reaction with significant charge and mass rearrangements, including many reaction channels such as quasielastic scattering, deep-inelastic scattering, and quasifission. These processes are characterized by a large number of productions and wide angular distributions, which make it more challenging to identify the nucleus of interest from the other numerous products. Despite these challenges, there have been many experimental advances in the study of MNT reactions [5–11]. It is demonstrated that the cross sections produced by MNT reactions are several orders of magnitude higher than those produced by projectile fragmentation for the $N = 126$ nuclei [7]. The ^{216,241}U, ^{219}Np, ^{223,229}Am, and ^{233}Bk were synthesized successively within ten years by MNT reactions [12,13]. Additionally, it was pointed out that new activities with Z as high as 116 are possibly produced in MNT reactions with the aid of the energies and half-lives of α emitters [14].

In addition, theorists have built confidence in the capability of MNT reactions to produce neutron-rich nuclei. Till now, the cross sections of MNT reactions have been predicted by several theoretical models, including the dinuclear system (DNS) model [15–18], the Langevin-type dynamical models [19–21], the GRAZING model [22–24], the CWKB model [25], the improved quantum molecular dynamics model (ImQMD) [26–28], the time-dependent Hartree-Fork (TDHF) theory [29,30], and so on. Based on the DNS model, it was suggested that the production cross sections of neutron-rich nuclei around the $N = 126$ closed-shell were higher when the radioactive beam ^{144}Xe was used to impinge on ^{208}Pb compared to using the ^{136,139}Xe beam [18]. Another study

*wenpeiwei@hotmail.com
†cjlin@ciae.ac.cn
‡xinxing@impcas.ac.cn

based on the ImQMD model investigated the reaction of ^{136}Xe + ^{198}Pt [28], which showed that the reaction can produce more than 50 new neutron-rich nuclei with cross sections larger than 10^{-6} mb.

Many dissipative physical phenomena, including the electrical field in a laser, atom implantation in metal, and dissipative heavy-ion reactions, can be understood in terms of Brownian motion [31]. Equations of motion like the Langevin equation can be used to explain the distribution functions of Brownian motion, which has proved to be an effective tool for exploring low-energy heavy-ion reactions involving transfer, deep-inelastic scattering, fusion, and fission processes [32–37]. As mentioned in Ref. [32], it is beneficial to describe the transfers of neutrons and protons by solving the master equation for the distribution function. However, it cannot be used directly in a common set of coupled differential equations for coordinates like distance and deformation. By applying specific rules, the equation for nuclei rearrangement can be transformed into the Langevin equation for the mass asymmetry degree of freedom. In many studies using multidimensional Langevin dynamics, the mass asymmetry or its equivalent variant is usually adopted as one necessary degree of freedom, which changes continuously during evolution. However, charge asymmetry is often not considered, partly due to its complexity [32–36]. As a consequence, these models can only predict the mass distribution but not the charge distribution. References [19,21,38] attempted to construct an extra independent charge asymmetry degree to represent the changes of proton number in fusion and the MNT reactions, which is similar in form to the evolution of the mass asymmetry.

In our previous work, we developed a dynamical dinuclear system model for MNT reactions that combines radial dynamics and random transfer processes during the dinuclear evolution [39]. The equation of radial motion and the master equation governing the transfer process are solved iteratively. The solving of the master equation is based on the Monte Carlo method, where the proton and neutron are transferred randomly. The model could describe both quasielastic and deep-inelastic transfers, yielding promising results. However, the dynamical deformations and thermal fluctuations during the radial evolution, like those in the multidimensional Langevin equation, were not considered. The HICOL model, abbreviated as heavy-ion collisions, was proposed in Ref. [40], which is a three-dimensional Langevin model based on the one-body dissipative approach to describe the deep-inelastic process. This model, including dynamical deformations and the mass asymmetry, was used in many subsequent studies on fusion and fission reactions [41–43]. However, since the thermal fluctuations are not included in this model, typically only the mean trajectories predicted by it are used to gain insight into the reaction dynamics. Besides, there is no explicit cross section output in this model, so it has not been used in comparisons with recent experimental MNT reaction cross sections.

To properly estimate the final cross sections, in this letter, we propose a model named the CLIM-H model. Furthermore, we incorporate thermal fluctuations into the model. Instead of using GEMINI for the de-excitation of fragments, CLIM-H is linked with GEMINI++ to calculate the de-excited cross sections [44,45]. It is expected that the description of the MNT reactions could be improved. The MNT reaction involving nuclei Pb will be studied, which is often used in literature for the synthesis of $N = 126$ nuclei. The isotope distributions for ^{58,64}Ni + ^{208}Pb, as well as the angular and isotope distributions of the recently measured ^{206}Pb + ^{118}Sn, will be investigated in depth for the test of this method.

II. METHODS

In this theoretical framework, we solve the equation of radial motion and the master equation for the general dinuclear system iteratively. The transport master equation at different excitation energies and angular momenta governing the mass and charge distributions among the fragments is

$$\begin{aligned}\frac{\partial}{\partial t}P_{Z,N}(t) = {} & \Delta^{(-,0)}_{Z+1,N}P_{Z+1,N}(t) + \Delta^{(+,0)}_{Z-1,N}P_{Z-1,N}(t) \\ & + \Delta^{(0,-)}_{Z,N+1}P_{Z,N+1}(t) + \Delta^{(0,+)}_{Z,N-1}P_{Z,N-1}(t) \\ & - \left(\Delta^{(-,0)}_{Z,N} + \Delta^{(+,0)}_{Z,N} + \Delta^{(0,-)}_{Z,N} + \Delta^{(0,+)}_{Z,N}\right)P_{Z,N}(t),\end{aligned} \tag{1}$$

where the charge, neutron, and mass numbers are denoted as $Z_P = Z$, $N_P = N$, and $A_P = Z + N$ for the projectile-like nucleus, and $Z_T = Z_{\rm tot} - Z_P$, $N_T = N_{\rm tot} - N_P$, and $A_T = A_{\rm tot} - A_P$ for the target-like nucleus. $P_{Z,N}(t)$ is the probability of finding the general dinuclear system in the state (Z, N) at time t. In this equation, we take only transitions $Z \leftrightharpoons Z \pm 1$, $N \leftrightharpoons N \pm 1$ into account. The transition coefficients of the $\Delta_{Z,N}$ for cases of plus or minus one proton or neutron are calculated as $p_0(r)/\tau$, where the collision time τ is determined by the width $\hbar\omega_0$ according to the formula $\tau = 1/\omega_0$. We adopt the energy-dependent transfer probability similar to those in Refs. [22,46], namely,

$$p_0(r) = \frac{2\pi/(\hbar\omega_0)^2}{1 + \exp[2\kappa(r - r_0)]} \exp\left[-\left(\frac{Q - Q_{\rm opt}}{\hbar\omega_0}\right)^2\right], \tag{2}$$

where r_0 is the distance of the closest approach and Q is the binding energy difference from ground state to ground state. The wave number κ is the average exponential slope of the single-particle wave function of the projectile nucleus and the target nucleus, which is $\sqrt{M(-\epsilon_{\rm F})/2\hbar^2} + \sqrt{M(-\epsilon'_{\rm F})/2\hbar^2}$ for the neutron, and

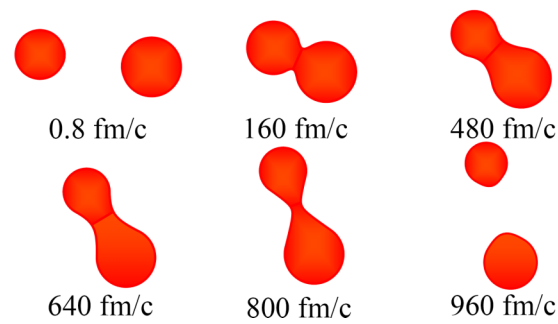

FIG. 1. The development of the ^{206}Pb + ^{118}Sn composite system's form given by CLIM-H with $L = 100\hbar$ at the indicated time.

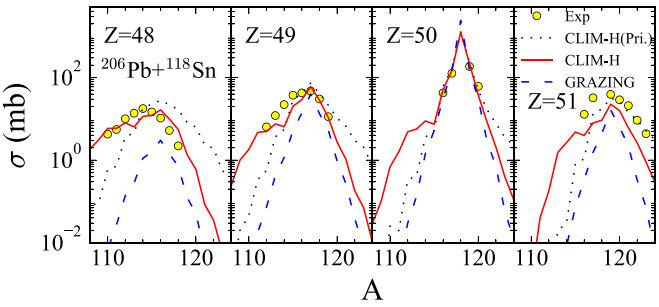

FIG. 2. Target-like isotopic production cross sections for reaction $^{206}\mathrm{Pb}+{}^{118}\mathrm{Sn}$ at $E_{\mathrm{c.m.}}=437$ MeV. The solid lines, dotted lines, and dashed lines represent the theoretical results provided by the CLIM-H model, the CLIM-H model without GEMINI + +, and the GRAZING model. Solid circles represent experiment results [11].

$\sqrt{M(-\epsilon_{\mathrm{F}}+Z_T e^2/R_T)/2\hbar^2}+\sqrt{M(-\epsilon'_{\mathrm{F}}+Z_P e^2/R_P)/2\hbar^2}$ for the proton. The R_P and R_T are the radius for the projectile and the target. The ϵ_{F} and ϵ'_{F} are the approximate separation energy for the projectile and the target. M is the nucleon mass. The optimum energy Q_{opt} is zero for neutron transfer, $(Z_P-Z_T)e^2/r_0$ for proton stripping, and $(Z_T-Z_P)e^2/r_0$ for proton pick-up. The average r_0 is $1.25(A_P^{1/3}+A_T^{1/3})$, which is similar for neutrons and protons [47,48]. The coefficient $(\hbar\omega_0)^2=\kappa\hbar^2\ddot{r}_0=\kappa\hbar^2(2E_{\mathrm{c.m.}}-V_B)/\mu R_B$ [46], where R_B and V_B are the Coulomb radius and Coulomb barrier, and μ is the reduced mass.

A large number of events for an impact parameter are calculated to determine the transfer cross section according to the final fragments. The kinetic Monte Carlo method is used to solve the master equation as that in our previous work [39]. For each impact parameter, it is performed in the following steps. At time t, we calculate the transition rates $\Delta_{Z_iN_i}$ from (Z,N) to all possible states (Z_i,N_i) with total state number as $S_{Z,N}$. Then we calculate the cumulative function $C_i=\Delta t\sum_{j=1}^{i}\Delta_{Z_jN_j}$ for $i=1,\ldots,S_{Z,N}$. The total rate is conserved to be one. After that a uniform random number $u\in(0,1]$ is obtained to find the state i for which $C_{i-1}<u\leqslant C_i$. Finally, the state i is chosen as the final state and solves the radial motion from t to $t+\Delta t$. The above procedures are carried out iteratively during the evolution and Δt is fixed as $0.4\,\mathrm{fm}/c$ in this study.

The radial dynamics part of the current model is based on the HICOL model [40]. It is assumed that the profile function is composed of a circle and a hyperbolic curve with ten parameters for bipartite shapes or eight parameters for single shapes. All of the parameters could be characterized by three collective degrees of freedom r, σ, and Δ, which represent the distance between two sphere centers, neck volume divided by total volume $\frac{R^3-R_T^3-R_P^3}{R^3}$ where R is the radius of the compound sphere, and radius asymmetry $(R_{\mathrm{P}}-R_{\mathrm{T}})/(R_{\mathrm{P}}+R_{\mathrm{T}})$, respectively. The colliding nuclei are considered to be incompressible Werner-Wheeler flows [49] allowing us to derive the collective velocity field and the inertia tensor m. The collective degrees of freedom q and their conjugate momenta p obey the general Langevin equations:

$$\frac{dq_i}{dt}=\sum_j(m^{-1})_{ij}p_j,$$
$$\frac{dp_i}{dt}=-\frac{\partial E_{\mathrm{kin}}}{\partial q_i}-\frac{\partial V}{\partial q_i}-\sum_j\gamma_{ij}(m^{-1}p)_j+\sum_j g_{ij}\Gamma_j(t), \tag{3}$$

where E_{kin} represents the kinetic energy. The Yukawa plus exponential double-fold potential energy V is adopted in

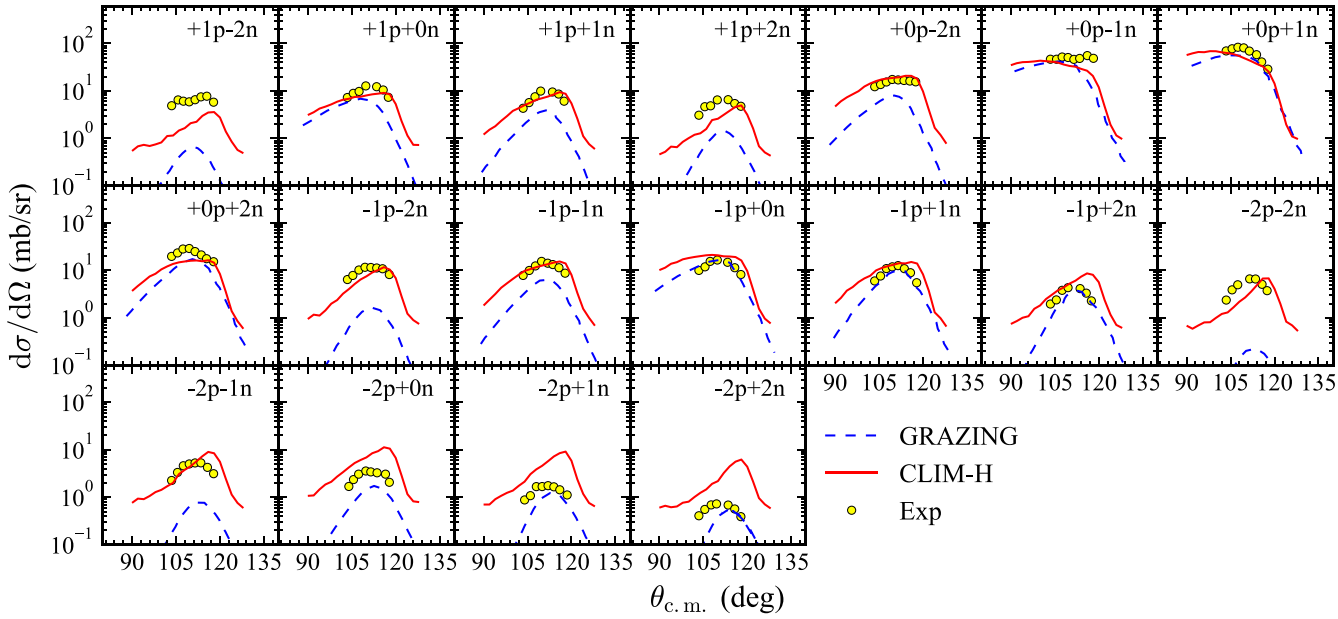

FIG. 3. Angular distributions of the $^{206}\mathrm{Pb}+{}^{118}\mathrm{Sn}$ reaction for the indicated transfer channels. Theoretical results by the GRAZING model and the CLIM-H model with GEMINI + + are shown as the dashed and the solid lines, respectively. The experimental data are taken from Ref. [11].

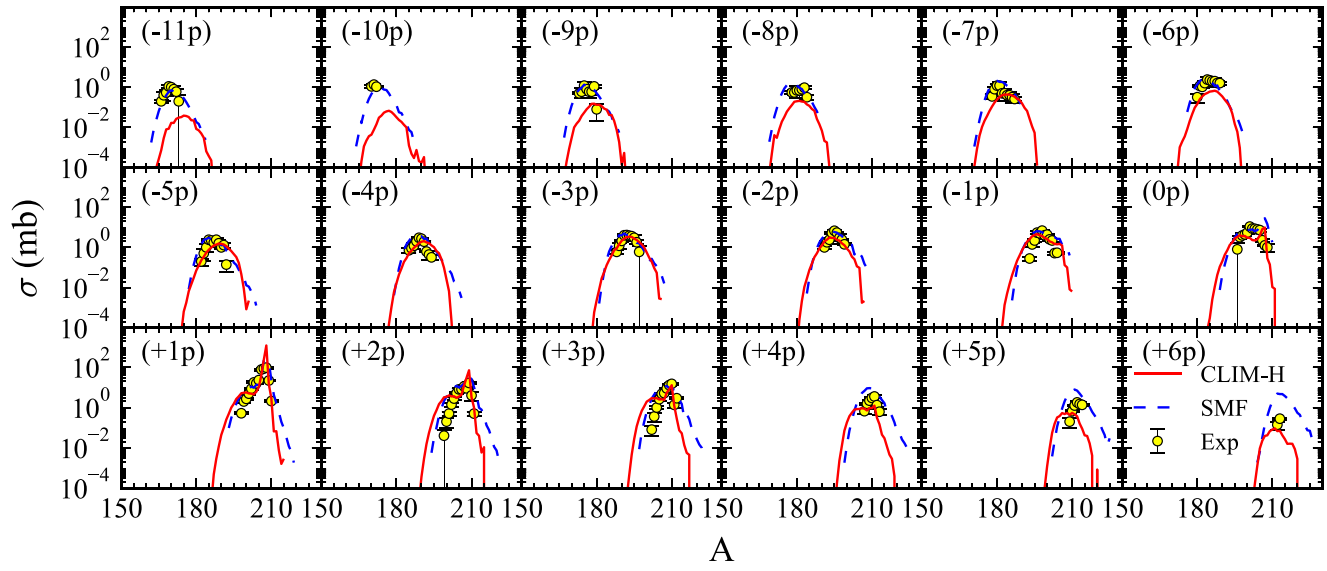

FIG. 4. Target-like isotopic production cross sections for reaction ^{64}Ni + ^{208}Pb at $E_{\mathrm{c.m.}} = 268$ MeV. The solid lines and dashed lines represent theoretical results provided by CLIM-H and SMF. Solid circles represent experiment results [50].

the current model. The coefficients in potential energy remain consistent with Eq. (3.37-44) in Ref. [40] except a_s. It is adjusted slightly as 23 MeV in the calculations to describe the peak position of the grazing angle. As for the strength of the random force g_{ij}, it meets the fluctuation-dissipation theorem by $\sum_k g_{ik}g_{jk} = \gamma_{ij}T$, where T is the mean temperature related to the heat energy and γ_{ij} denotes the friction tensor [34]. Dissipation in the model consists of wall dissipation and window dissipation. When the distance between two nuclei is not too small, window dissipation, also known as the particle exchange mechanism, can properly explain the major dissipative phenomena. Wall dissipation is used to explain the dissipation phenomena brought by the moving of single-particle potential at a closer distance.

It is worth noting that the radius asymmetry Δ is particularly critical as it serves as a connection between the master equation and the Langevin Equation. In our current CLIM model, we have modified the HICOL model's three-dimensional Langevin equation to a two-dimensional version, focusing on the independent collective variables r and σ. The variable Δ is derived by solving the master equation in Eq. (1). Once the numbers of protons and neutrons in the projectile-like and target-like fragments are determined, Δ can be calculated using the cubic equation derived from Eq. (3.103) in Ref. [40]:

$$A_{\mathrm{P}} = \frac{A_{\mathrm{tot}}}{2}\frac{(1+\Delta)^3}{1+3\Delta^2}, \tag{4}$$

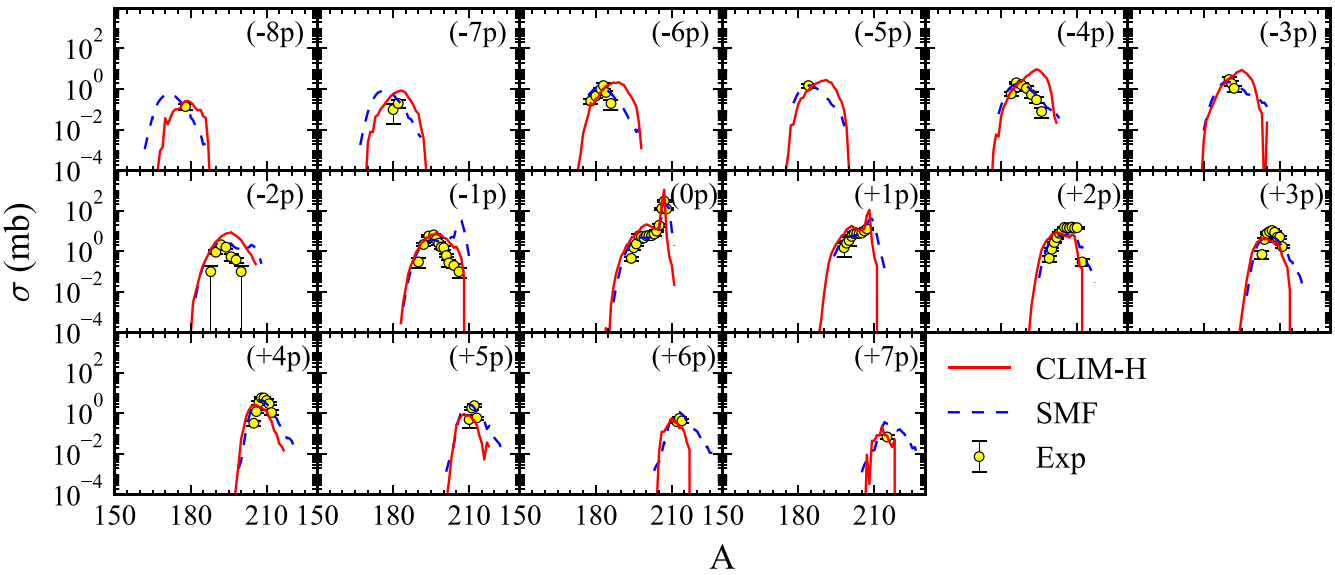

FIG. 5. Similar to those in Fig. 4 but for reaction ^{58}Ni + ^{208}Pb at $E_{\mathrm{c.m.}} = 270$ MeV. The experimental data are transformed from Ref. [52].

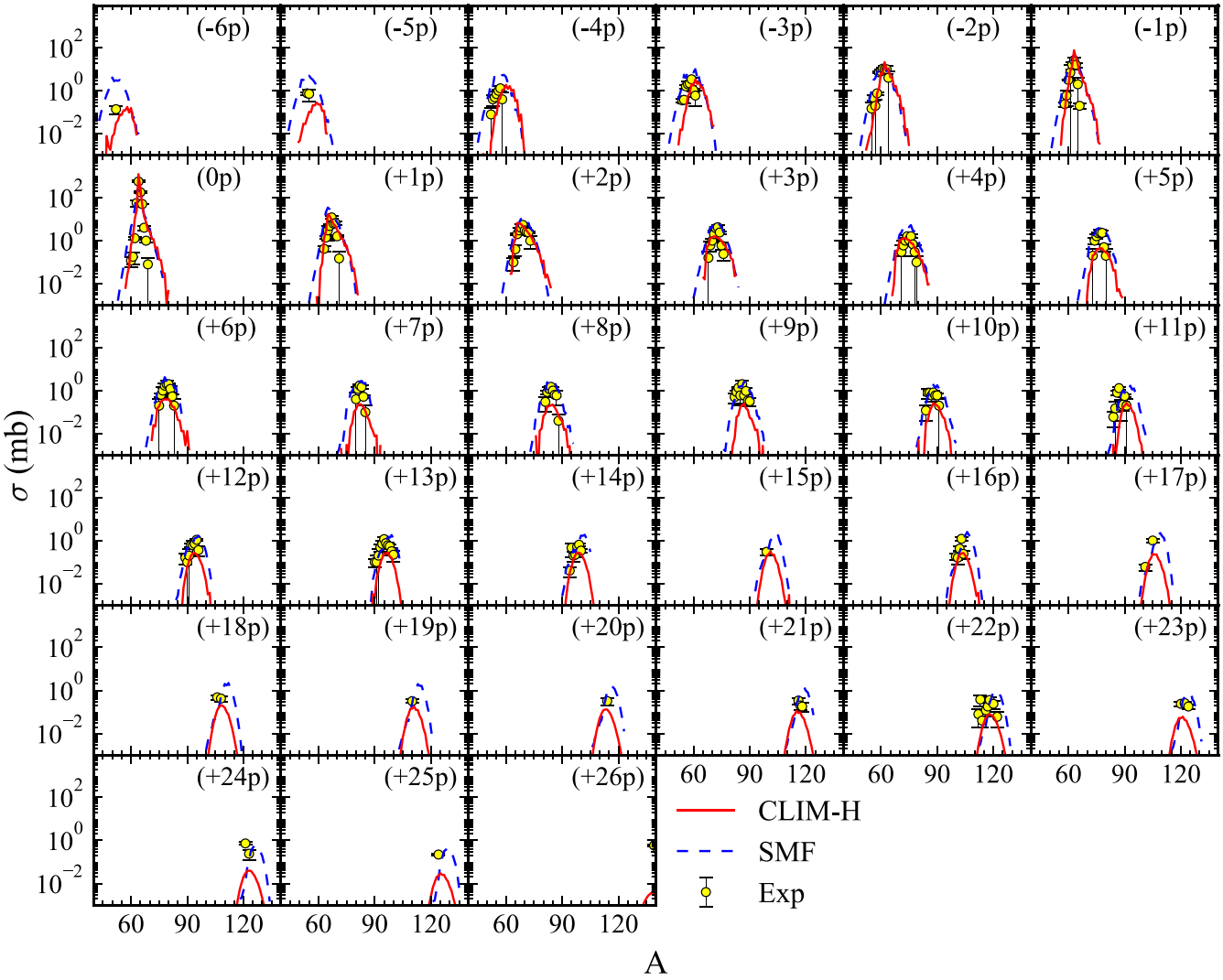

FIG. 6. Similar to those in Fig. 4 but for projectile-like isotopic production cross sections. The experimental data are transformed from Ref. [50].

which is

$$\Delta^3 + 3\left(1 - \frac{2A_{\rm P}}{A_{\rm tot}}\right)\Delta^2 + 3\Delta + 1 - \frac{2A_{\rm P}}{A_{\rm tot}} = 0, \qquad (5)$$

where $A_{\rm P} = Z_{\rm P} + N_{\rm P}$ and $A_{\rm tot} = Z_{\rm P} + N_{\rm P} + Z_{\rm T} + N_{\rm T}$ represent the mass numbers of the projectile-like fragments and the system, respectively. The unique real root of this equation indicates a one-to-one correspondence between $A_{\rm P}$ and Δ.

In summary, our process involves:

(1) Determining the variables $Z_{\rm P}$, $Z_{\rm T}$, $N_{\rm P}$, and $N_{\rm T}$ at time t by solving the master equation using Monte Carlo methods, which then allows us to calculate Δ using Eq. (4) in this document.

(2) Updating the reaction quantities such as shape, mass tensor, and frictions based on the newly derived Δ, and then solving the two-dimensional Langevin equation from time t to $t + \Delta t$ to obtain new values for r, σ. Other quantities like new momentum and kinetic energies could then be obtained.

(3) Repeating this procedure iteratively until the MNT process for that event is complete.

Consequently, we have named our theoretical framework CLIM, as it iteratively couples the Langevin dynamics with the master equation. This novel framework enables us to simultaneously address proton and neutron transfers other than solely the mass degree of freedom in the original HICOL model. The validity of the CLIM methods will undergo testing through comparisons with both experimental data and other theoretical models below.

III. ANALYSIS AND RESULTS

We take the MNT reaction ^{206}Pb + ^{118}Sn with the center of mass incident energy $E_{\rm c.m.} = 437$ MeV as a typical example. Figure 1 shows how the profile of the nucleus evolves during the collision process. The relative angular momentum L is set to $100\hbar$. At the initial moment of evolution, the initial deformation is not considered, and both nuclei are spherical. When it evolves to a certain moment, such as 640 fm/c, due to the influence of nuclear interaction and the set of profile functions, the two nuclei undergo large deformation at the contact

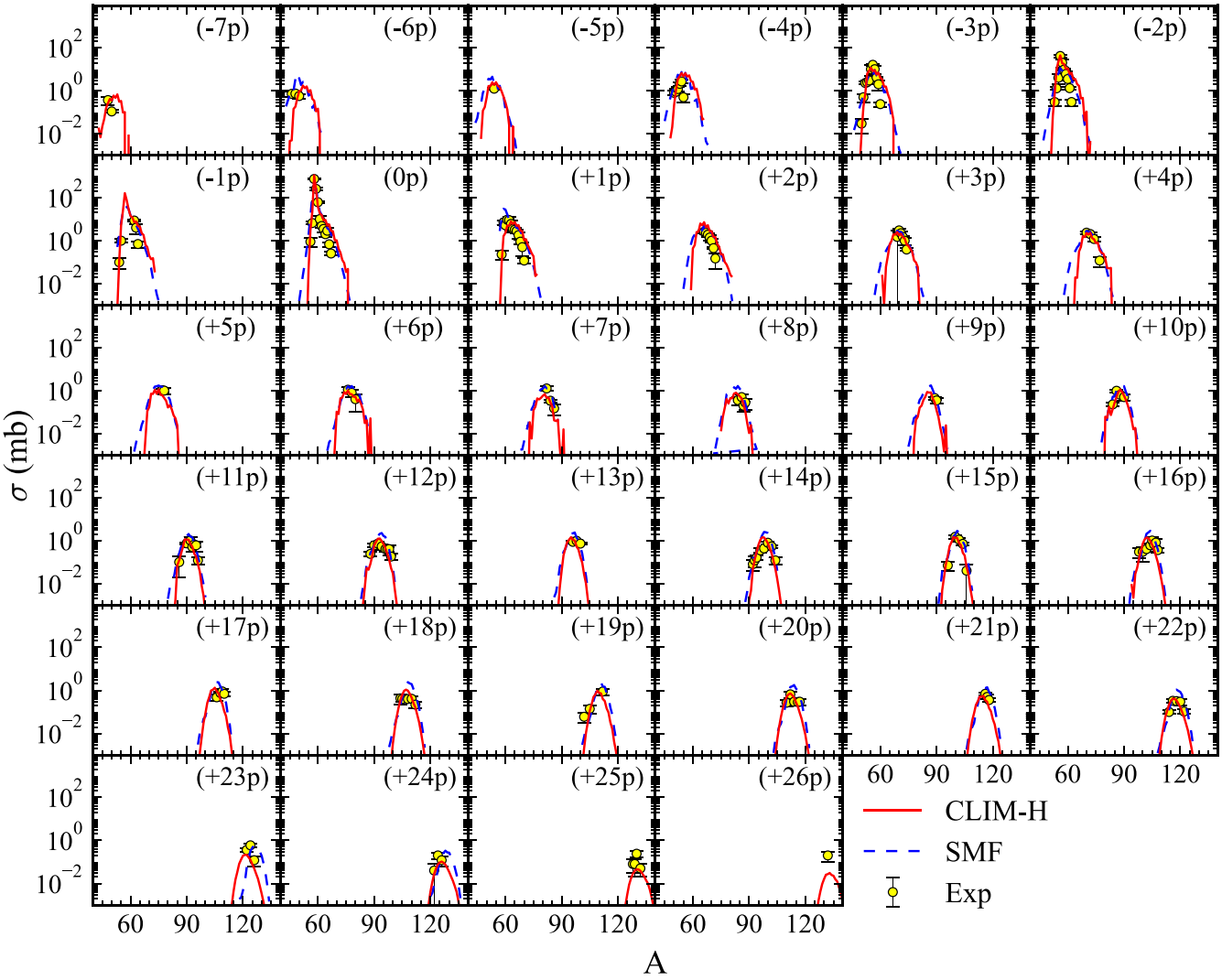

FIG. 7. Similar to those in Fig. 6 but for reaction $^{58}\mathrm{Ni} + {}^{208}\mathrm{Pb}$ at $E_{\mathrm{c.m.}} = 270$ MeV. The experimental data are transformed from Ref. [52].

distance, while still maintaining a spherical shape at the far end. When they separate at the last moment of evolution, such as 960 fm/c, the two nuclei return to their spherical shape.

Most previous theoretical work made calculations and predictions on the total production cross sections of MNT fragments, which represent the integrated values of angular distributions and energy over their entire range. This is suitable for experiments such as those measured with the γ coincidence analysis, which does not depend on the angle coverage of the detectors.

However, to describe experiments such as those performed at the large solid angle magnetic spectrometer PRISMA of Legnaro National Laboratory, one should take into account the position of the detector since they are usually placed at a certain angular range. The MNT reaction $^{206}\mathrm{Pb} + {}^{118}\mathrm{Sn}$ with the center of mass incident energy $E_{\mathrm{c.m.}} = 437$ MeV was recently measured with the PRISMA [11]. The incident energy was 1.1 times the empirical Coulomb barrier [51]. The experiment detector was placed at two positions covering the angular range $20.5^\circ < \theta_{\mathrm{lab.}} < 28.5^\circ$ and $30.5^\circ < \theta_{\mathrm{lab.}} < 38.5^\circ$ according to Fig. 2 of Ref. [11]. We calculate the angular integrated cross sections and the angular distributions of target-like fragments for this reaction by using the current model within the angular range $20.5^\circ < \theta_{\mathrm{lab}} < 38.5^\circ$. The comparisons between the experiment results and the GRAZING model are shown in Figs. 2 and 3.

As we can see, the general trends of the differential cross section $d\sigma/d\Omega$ of each nucleus predicted by the CLIM-H model roughly match the results of the experiments. Moreover, compared to the results given by the GRAZING model, the cross sections calculated by the CLIM-H model are higher and closer to the experimental data in most cases. This is because GRAZING is better suited to compute the grazing collisions. The experiment grazing angle of this reaction is around 109°, which is also the experiment peak value for each case shown in Fig. 3. However, one could see that the theoretical peak angle of the CLIM-H calculations is around 120°. This means that attractive nuclear potential should be larger to decrease the theoretical grazing angle. It could also be seen that in some cases, the CLIM-H calculations are much lower than the experimental angular distributions. This could also be reflected in the angular integrated cross sections,

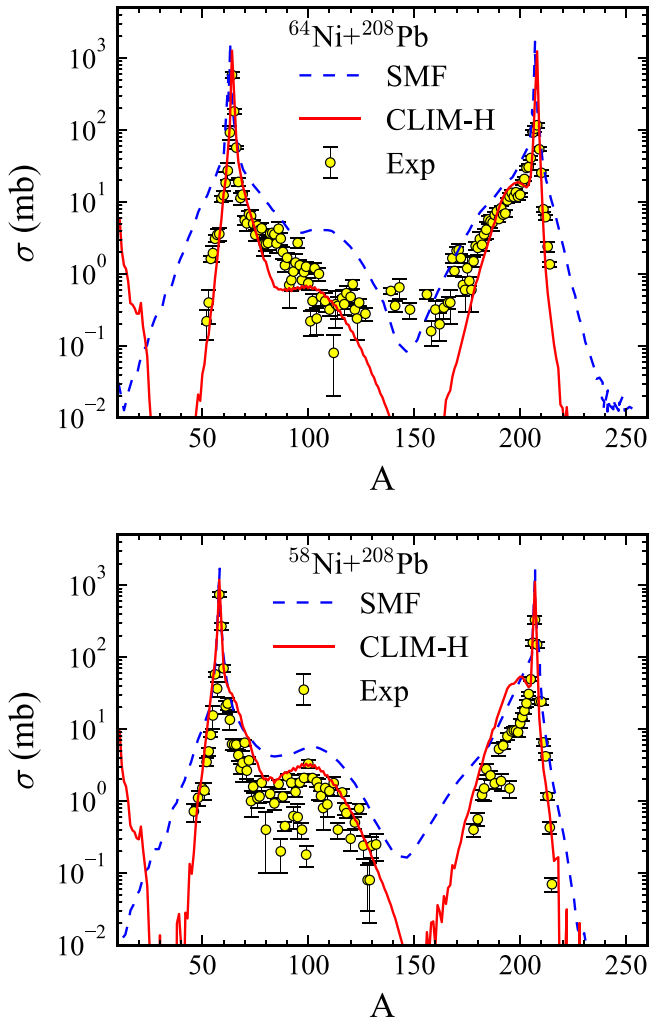

FIG. 8. Similar to those in Figs. 4–7 but for the mass distributions of ^{64,58}Ni + ^{208}Pb. The experimental data are transformed from Refs. [50,52]. In the $A \leqslant 30$ region, there are lots of de-excited products from heavy nuclei.

which have been given in Fig. 2. It could be seen that when $Z = 50$, the results of both the CLIM-H model and the GRAZING model coincide well with the experimental data. When there are more nucleons transferred at $Z = 48$, 49, and 51, both theoretical models underestimate the cross sections. The results of the CLIM-H model are closer to the experiment due to considering deeper collisions than the GRAZING model. However, they are still lower than the experiment data in cases like the left side of the peak at $Z = 48$–49, which might be caused by the evaporation of neutrons from other nuclei with larger excitation energies. This can be attributed to the fact that the amplitude and distribution of the excitation energy between the fragments might not be fully appropriate yet. We will try to improve the potential and other details of the CLIM-H model in the following works.

Figures 4 and 5 display the experimental and theoretical target-like secondary production cross sections of ^{64}Ni, ^{58}Ni + ^{208}Pb reactions at $E_{\text{c.m.}} = 268$, 270 MeV, respectively. Similarly, their projectile-like secondary production cross sections are shown in Figures 6 and 7. The stochastic mean-field (SMF) model is built on top of the three-dimensional TDHF results and especially considers the quantum diffusion, which is clarified to be more applicable to describe the MNT reaction in Ref. [30]. For the $(+xp)$ channel shown in Figs. 4 and 5, the CLIM-H model produces similar results to those produced by the SMF approach, which are all closed to the experimental data. As for several reaction channels in the $(-xp)$ channels such as the cases of $Z = 78$–81, there is an outstanding agreement between the CLIM-H model and experiment data for ^{64}Ni + ^{208}Pb. As a contrast, the SMF approach evidently overestimates the width of isotopic distributions, which partly owes to the linearization of the Langevin equation in obtaining the variance and the covariance of neutron and proton numbers [30]. Our results are narrower in the isotopic distributions, which is also comparable with the experimental data for many cases. For reaction ^{58}Ni + ^{208}Pb, the results of the CLIM-H model and the SMF model are similar to the experimental data. However, it should be noted that the experimental data for this reaction are less complete than the other due to the lack of the off-line radioactivity measurement [52]. In addition, for the projectile-like fragments shown in Figs. 6 and 7, the calculations of the CLIM-H model agree also with most of the experimental data, which are similar to the results of the SMF model but with a relatively narrower distribution width.

The contrast between the results of the two models and the experimental results is more obvious in the mass distribution, which is shown in Fig. 8 for these two reactions. The distribution widths of the SMF model are generally larger than the experimental data at almost the whole mass range. The current model calculations are closer to the experimental results near the peaks on both sides, but lower in the middle for reaction ^{64}Ni + ^{208}Pb. This is due to the fact that the separation after capture or the fission of the heavy nuclei is not well treated in the CLIM-H model, which could be better described in the DNS model as in Ref. [53]. The lightest already known isotone with $N = 126$ is ^{202}Os with $Z = 76$. The next $N = 126$ neutron-rich nuclei that researchers are very concerned about are ^{200}W ($Z = 74$), and ^{201}Re($Z = 75$). The SMF model predicts that the cross sections of these two nuclides can reach more than 10^{-4} mb shown in Fig.12 of Ref. [30]. However, in the calculations of the CLIM-H model, no appreciable production cross sections are found for these two nuclei. More systematic studies should be performed in the future to find the optimum reactions for producing $N = 126$ nuclei.

IV. CONCLUSION

In summary, a approach for MNT reactions is developed namely the CLIM-H model. The model incorporates the use of kinetic Monte Carlo methods to solve the master equations for the proton and neutron self-consistently. The parametrized exponential transfer probability is adopted similarly to that in the GRAZING model. Compared to the results of the GRAZING model, the outcomes of the CLIM-H model could depict the experimental angular distributions of reaction ^{206}Pb + ^{118}Sn, as well as the isotope distributions. The isotope distributions and mass distributions given on the system ^{58}Ni, ^{64}Ni + ^{208}Pb are also more consistent with experiments when compared to the results provided by the SMF model. Going forward, we

envisage the following aspects to improve the transfer probability, such as considering its dependence on the excitation energy or obtaining them from the microscopic two-center shell model. We will also systematically calculate more MNT reactions to find out the optimum system and energy to produce $N = 126$ nuclides, as well as give the angular and energy distribution appropriate for detection. Besides, as a general approach, the CLIM approach based on another dynamical model like TORINO will also be studied to test the multipole dynamical deformations [54]. At the submission of this paper, we noticed Prof. Zhu has also a similarly developed theoretical framework by combining the Langevin equation and master equation [55]. The unique aspect of this approach is its capability to calculate the mass distribution and the charge distribution in a self-consistent manner. This feature can serve as a valuable reference for other studies that employ the multidimensional Langevin equation considering solely the mass asymmetry degree of freedom.

ACKNOWLEDGMENTS

We would like to acknowledge Prof. L. Zhu, Prof. L.L. Liu, and Prof. C. Li for the important discussions which significantly improve this work. This work is supported by the Strategic Priority Research Program of Chinese Academy of Sciences under Grant No. XDB34010300, the National Key R&D Program of China (Contract No. 2022YFA1602302), the National Natural Science Foundation of China (Grants No. 12022501, No. 12105329, No. 12235020, No. 12375130, No. 12275360, No. 12175314, No. 12175313, and No. U2167204), the Continuous-Support Basic Scientific Research Project, the Young Talent Development Foundation (Grant No. YC212212000101), the Leading Innovation Project (Grants No. LC192209000701, No. LC202309000201), and the project supported by the Director's Foundation of Department of Nuclear Physics, China Institute of Atomic Energy (12SZJJ-202305).

[1] O. Sorlin and M.-G. Porquet, Prog. Part. Nucl. Phys. **61**, 602 (2008).
[2] C. Y. Wu, W. V. Oertzen, D. Cline, and M. W. Guidry, Annu. Rev. Nucl. Part. Sci. **40**, 285 (1990).
[3] L. Corradi, G. Pollarolo, and S. Szilner, J. Phys. G: Nucl. Part. Phys. **36**, 113101 (2009).
[4] O. Beliuskina *et al.*, Eur. Phys. J. A **50**, 161 (2014).
[5] S. Szilner *et al.*, Phys. Rev. C **71**, 044610 (2005).
[6] S. Szilner *et al.*, Phys. Rev. C **76**, 024604 (2007).
[7] Y. X. Watanabe *et al.*, Phys. Rev. Lett. **115**, 172503 (2015).
[8] A. Vogt *et al.*, Phys. Rev. C **92**, 024619 (2015).
[9] T. Mijatović, S. Szilner, L. Corradi, D. Montanari, G. Pollarolo, E. Fioretto, A. Gadea, A. Goasduff, D. J. Malenica, N. Marginean, M. Milin, G. Montagnoli, F. Scarlassara, N. Soic, A. M. Stefanini, C. A. Ur, and J. J. Valiente-Dobon, Phys. Rev. C **94**, 064616 (2016).
[10] F. Galtarossa *et al.*, Phys. Rev. C **97**, 054606 (2018).
[11] J. Diklić S. Szilner, L. Corradi, T. Mijatovic, G. Pollarolo, P. Colovic, G. Colucci, E. Fioretto, F. Galtarossa, A. Goasduff, A. Gottardo, J. Grebosz, A. Illana, G. Jaworski, M. J. Gomez, T. Marchi, D. Mengoni, G. Montagnoli, D. Nurkic, M. Siciliano, N. Soic, A. M. Stefanini, D. Testov, J. J. Valiente-Dobon, and N. Vukman, Phys. Rev. C **107**, 014619 (2023).
[12] H. Devaraja *et al.*, Phys. Lett. B **748**, 199 (2015).
[13] T. Niwase *et al.*, Phys. Rev. Lett. **130**, 132502 (2023).
[14] S. Wuenschel *et al.*, Phys. Rev. C **97**, 064602 (2018).
[15] G. G. Adamian, N. V. Antonenko, and A. S. Zubov, Phys. Rev. C **71**, 034603 (2005).
[16] Z.-Q. Feng, G.-M. Jin, and J.-Q. Li, Phys. Rev. C **80**, 067601 (2009).
[17] Z.-Q. Feng, Phys. Rev. C **95**, 024615 (2017).
[18] L. Zhu, J. Su, W.-J. Xie, and F.-S. Zhang, Phys. Lett. B **767**, 437 (2017).
[19] V. Zagrebaev and W. Greiner, Phys. Rev. Lett. **101**, 122701 (2008).
[20] V. Zagrebaev and W. Greiner, Nucl. Phys. A **834**, 366c (2010).
[21] A. V. Karpov and V. V. Saiko, Phys. Rev. C **96**, 024618 (2017).
[22] A. Winther, Nucl. Phys. A **572**, 191 (1994).
[23] A. Winther, Nucl. Phys. A **594**, 203 (1995).
[24] P. W. Wen, C. Li, L. Zhu, C. J. Lin, and F. S. Zhang, J. Phys. G: Nucl. Part. Phys. **44**, 115101 (2017).
[25] E. Vigezzi and A. Winther, Ann. Phys. **192**, 432 (1989).
[26] C. Li, F. Zhang, J. Li, L. Zhu, J. Tian, N. Wang, and F. S. Zhang, Phys. Rev. C **93**, 014618 (2016).
[27] N. Wang and L. Guo, Phys. Lett. B **760**, 236 (2016).
[28] C. Li *et al.*, Phys. Lett. B **776**, 278 (2018).
[29] K. Sekizawa, Phys. Rev. C **96**, 014615 (2017).
[30] K. Sekizawa and S. Ayik, Phys. Rev. C **102**, 014620 (2020).
[31] H. Risken, *The Fokker-Planck Equation: Methods of Solution and Applications*, 2nd ed. (Springer, Berlin/Heidelberg, 1996)
[32] V. Zagrebaev and W. Greiner, J. Phys. G: Nucl. Part. Phys. **31**, 825 (2005).
[33] Y. Huang, Y. Feng, E. Xiao, X. Lei, L. Zhu, and J. Su, Phys. Rev. C **106**, 054606 (2022).
[34] L.-L. Liu, X. Z. Wu, Y. J. Chen, C. W. Shen, Z. X. Li, and Z. G. Ge, Phys. Rev. C **99**, 044614 (2019).
[35] Z.-H. Liu and J.-D. Bao, Phys. Rev. C **87**, 034616 (2013).
[36] Y. Aritomo and S. Chiba, Phys. Rev. C **88**, 044614 (2013).
[37] J. Tian, N. Wang, and W. Ye, Phys. Rev. C **95**, 041601(R) (2017).
[38] J. Blocki, O. Mazonka, J. Wilczynski, Z. Sosin, and A. Wieloch, Acta. Phys. Pol. B **31**, 1513 (2000).
[39] P. W. Wen, A. K. Nasirov, C. J. Lin, and H. M. Jia, J. Phys. G: Nucl. Part. Phys. **47**, 075106 (2020).
[40] H. Feldmeier, Rep. Prog. Phys. **50**, 915 (1987).
[41] K. Siwek-Wilczyńska, J. Wilczyński, R. H. Siemssen, and H. W. Wilschut, Phys. Rev. C **51**, 2054 (1995).
[42] S. Appannababu *et al.*, Phys. Rev. C **94**, 044618 (2016).
[43] P. N. Patil *et al.*, Phys. Rev. C **102**, 034618 (2020).
[44] D. Mancusi, R. J. Charity, and J. Cugnon, Phys. Rev. C **82**, 044610 (2010).
[45] P. W. Wen *et al.*, Phys. Rev. C **99**, 034606 (2019).
[46] V. I. Zagrebaev, Phys. Rev. C **67**, 061601(R) (2003).
[47] A. Winther, Fisika **22**, 41 (1990).

[48] J. M. Quesada, G. Pollarolo, R. A. Broglia, and A. Winther, Nucl. Phys. A **442**, 381 (1985).
[49] K. T. R. Davies, A. J. Sierk, and J. R. Nix, Phys. Rev. C **13**, 2385 (1976).
[50] W. Królas *et al.*, Nucl. Phys. A **724**, 289 (2003).
[51] P. W. Wen *et al.*, Phys. Rev. C **105**, 034606 (2022).
[52] W. Królas *et al.*, Nucl. Phys. A **832**, 170 (2010).
[53] Z. Cheng and X. J. Bao, Phys. Rev. C **103**, 064613 (2021).
[54] C. Dasso and G. Pollarolo, Comput. Phys. Commun. **50**, 341 (1988).
[55] L. Zhu, Phys. Lett. B **849**, 138423 (2024).